Synthesis of 14-oxa-1,4,8,11-tetraazabicyclo[9.5.3]nonadecane (L1) and a Spectroscopic and Structural Study of [Ni(L1)(ClO_4)](ClO_4) and of the Macrobicyclic Precursor Diamide Complex, [Ni(HL2)](ClO_4); Chloride Substitution Kinetics of the Corresponding $[Ni(III)(L1)]^{3+}$ Species

M. Rodopoulos,[†] T. Rodopoulos,[‡] J. N. Bridson,[§] L. I. Elding,[||] S. J. Rettig,[⊥] and A. McAuley*,[#]

CSIRO Molecular Science, Clayton South, Victoria, Australia, CSIRO Minerals, Clayton South, Victoria, Australia, Department of Chemistry, Memorial University of Newfoundland, St. John's, Newfoundland, Canada, Inorganic Chemistry, Chemical Center, Lund University, Lund, Sweden, Chemistry Department, University of British Columbia, Vancouver, British Columbia, Canada, Department of Chemistry, University of Victoria, Victoria, British Columbia, Canada V8W 3V6

Received October 20, 2000

The pentadentate ligand 14-oxa-1,4,8,11-tetraazabicyclo[9.5.3]nonadecane (L1) has been synthesized by the high dilution cyclization of 1-oxa-4,8-diazacyclododecane ([10]aneN_2O) (**1**) with 1,3-bis(α-chloroacetamido)propane (**2**) and subsequent reduction of the diamide intermediate. The structure [Ni(L1)(ClO_4)](ClO_4) ($P2_1/c$ (no. 14), a = 8.608(3), b = 16.618(3), c = 14.924(4) Å, β = 91.53(3)° converged at R = 0.050 (R_w = 0.046) for 307 parameters using 2702 reflections with $I > 2\sigma(I)$. For the nickel(II) complex of the (monodeprotonated) precursor diamide ligand 14-oxa-1,4,8,11-tetraazabicyclo[9.5.3]nonadecane-3,9-dione (H_2L2), [Ni(HL2)](ClO_4) (*Pbca* (no. 61), a = 15.1590(3), b = 13.235(2), c = 18.0195(6) Å), the structure converged at R = 0.045 (R_w = 0.038) for 265 parameters using 1703 reflections with $I > 3\sigma(I)$. In the reduced system, the cyclam-based ligand adopts a *trans*-III configuration. The [Ni(L1)(ClO_4)]$^{2+}$ ion is pseudooctahedral with the Ni−O(ether) 2.094(3) Å distance shorter than the Ni−O(perchlorate) 2.252(4) Å. The nickel(II) and nickel(III) complexes are six-coordinate in solution. Oxidation of [Ni(L1)(OH_2)]$^{2+}$ with $K_2S_2O_8$ in aqueous media yielded an axial d^7 Ni(III) species ($g_\perp$ = 2.159 and $g_\perp$ = 2.024 at 77 K). The [Ni(L1)(solv)]$^{2+}$ ion in CH_3CN showed two redox waves, $Ni^{II/I}$ (an irreversible cathodic peak, $E_{p,c}$ = −1.53 V) and $Ni^{III/II}$ ($E_{1/2}$ = 0.85 V (reversible)) vs Ag/Ag^+. The complex [Ni(HL2)](ClO_4) displays square-planar geometry with monodeprotonation of the ligand. The ether oxygen is not coordinated. Ni−O(3) = 2.651(6) Å and Ni−O(3a) = 2.451(12) Å, respectively. The $Ni^{III/II}$ oxidation at $E_{1/2}$ = 0.24 V (quasi-reversible) vs Ag/Ag^+ is considerably lower than the saturated system. The kinetics of Cl^- substitution at [Ni(L1)(solv)]$^{3+}$ are pH dependent. Detachment of the ether oxygen atom is proposed, with insertion of a protonated water molecule which deprotonates at a pK_a more acidic than in the corresponding cyclam complex. Mechanistic implications are discussed.

Introduction

The coordination chemistry of the 14-membered tetraaza ligand cyclam (cyclam = 1,4,8,11-tetraazacyclotetradecane) has been studied extensively[1−6] owing to its capacity to bind, via various conformational isomers,[7] a wide range of transition metal ions, forming complexes of considerable thermodynamic stability and kinetic inertness. Previous reports[8−11] presented details of the synthesis of the macrobicyclic pentacoordinate ligands, L3−L5, in which a $-CH_2-CH_2-X-CH_2-CH_2-$ group (X = NH, O, S) bridges the 1,4 nitrogen atoms of the 14-membered tetraazacyclam ring. The L3−L5 cations (M^{n+} = Ni(II),

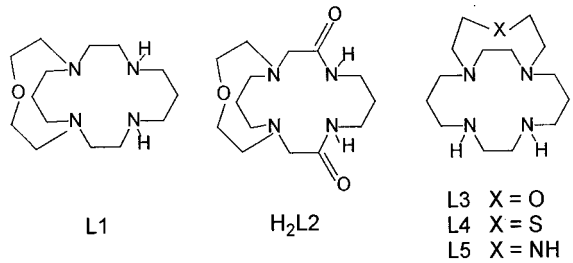

* To whom correspondence should be addressed.
[†] CSIRO Molecular Science.
[‡] CSIRO Minerals.
[§] Memorial University of Newfoundland.
[||] Lund University.
[⊥] University of British Columbia.
[#] University of Victoria.

(1) Cabbiness, D. K.; Margerum, D. W. *J. Am. Chem. Soc.* **1969**, *91*, 6540.
(2) Fabrizzi, L. *Comments Inorg. Chem.* **1985**, *4*, 33.
(3) Melson, G. A., Ed. *Coordination Chemistry of Macrocyclic Compounds*; Plenum Press: New York, 1979.
(4) Lindoy, L. *Chemistry of Macrocyclic Ligand Complexes*; Cambridge University Press: Cambridge, England, 1989.
(5) Hancock, R. D.; Martell, A. E. *Chem. Rev.* **1989**, *89*, 1875. Hancock, R. D. *J. Chem. Educ.* **1992**, *69* (8), 615.
(6) Busch, D. H. *Acc. Chem. Res.* **1978**, *11*, 392. Busch, D. H. *Adv. Chem. Ser.* **1971**, No. 100, 44.
(7) Bosnich, B.; Poon, C. K.; Tobe, M. L. *Inorg. Chem.* **1965**, *4*, 1102.
(8) Fortier, D. G.; McAuley, A. *Inorg. Chem.* **1989**, *28*, 655.
(9) Fortier, D. G.; McAuley, A. *J. Am. Chem. Soc.* **1990**, *112*, 2640.
(10) (a) Beveridge, K. A.; McAuley, A.; Xu, C. *Inorg. Chem.* **1991**, *30*, 2074. (b) Rodopoulos, T. Unpublished observations.
(11) McAuley, A.; Fortier, D. F.; Macartney, D. H.; Whitcombe, T. W.; Xu, C. *J. Chem. Soc., Dalton Trans.* **1994**, 2071.

10.1021/ic001163r CCC: $20.00
Published on Web 05/11/2001

Cu(II)) adopt a *trans*-I conformation in the solid state. A detailed analysis has been presented recently of all nickel 14-membered macrocycles in the Cambridge database,[12] showing that the majority of *trans*-I species are square planar or square pyramidal, and the *trans*-III conformation is associated with octahedral symmetry. Also, N-alkylation appears to confer additional thermodynamic stability to the *trans*-I configuration.[13]

The coordination properties of ether donors are of interest, particularly in contrasting the ligation of alkali metals with the first-row transition ions. This paper reports the synthesis of the macrobicycle L1, a structural isomer of L3. Since the electronic nature of each N_4O donor set is identical, any differences in the resulting coordination properties might be attributed principally to structural and kinetic effects.

Experimental Section

^{1}H and ^{13}C NMR spectra were recorded on Bruker WM250 or Bruker AC300 high field spectrometers with $CDCl_3$ as solvent. Mass spectra of the ligands were recorded on a Finnegan 330 GC−MS instrument by methane chemical ionization and electron impact techniques, and the metal complexes were recorded on a Kratos Concept spectrometer by FAB using *m*-NBA as medium or electrospray ionization. IR spectra were recorded on either a Bruker IFS25 (FTIR) or a Perkin-Elmer 1330 instrument, and UV−vis spectra were recorded on a Cary 5 UV−vis−NIR spectrophotometer. EPR spectra of solutions were recorded at ambient temperature and as frozen glasses at 77 K on a Varian E-6S EPR spectrometer using DPPH, $g = 2.0037$, as an external reference standard. Canadian Microanalytical Services, Delta, BC, Canada, determined elemental analyses. Electrochemical measurements were made on a Princeton Applied Research Model 273 potentiostat−galvanostat, interfaced with an IBM PC microcomputer, and data were recorded using the corrWare program (Scribner Associates Inc). The electrochemical cell employed a three-electrode configuration with platinum working and counter electrodes and $Ag/AgNO_3$ as reference electrode in 0.1 M Bu_4NClO_4 background electrolyte in CH_3CN. The half-wave potential, $E_{1/2}$, of the reference Fc/Fc^+ couple was measured at 0.10 V under the same experimental conditions.

An Applied Photophysics DX-17MV stopped-flow spectrophotometer interfaced with an Acorn microcomputer was used for studying the substitution kinetics. The $[Ni(III)(L1)]^{3+}$ solutions were prepared in situ by oxidation of the corresponding Ni(II) complex using a stoichiometric deficiency of $Co^{3+}(aq)$ in 3.89 M $HClO_4$. The ionic strength of all solutions was maintained at 1.0 M with the appropriate concentrations of $LiClO_4$ and $HClO_4$. The rate constants were measured under pseudo-first-order conditions in excess LiCl. Reaction kinetics were followed by monitoring the absorbance change due to chloride complex formation over the range 280−430 nm. Spectrophotometric determination of the pK_a of the $[Ni(III)(L1)]^{3+}$ species was made by measuring changes over the range 280−400 nm upon addition of microaliquots of $HClO_4$ to a $[Ni(III)(L1)]^{3+}$ solution at 283 K.

Synthesis. Caution: metal perchlorates are hazardous and should be used with care in only small quantities.

The ligand 1-oxa-4,8-diazacyclodecane, [10]-aneN_2O, (**1**) was prepared by the Richman and Atkins tosylate method,[14] with concentrated H_2SO_4 as detosylating agent. Synthesis of 1,3-bis(α-chloroacetamido)propane (**2**) used an adaptation of the method described by Bradshaw.[15]

14-Oxa-1,4,8,11-tetraazabicyclo[9.5.3]nonadecane-3,9-dione (H_2L2). Solutions of [10]-aneN_2O (**1**) (1.036 g, 7.183 mmol) (200 mL) and (**2**) (1.631 g, 7.183 mmol) (200 mL), both in dry acetonitrile, were added simultaneously over 38 h at 80 °C, with vigorous stirring under a dry nitrogen atmosphere using motor-driven syringes, to dry acetonitrile (2.5 L) containing suspended Na_2CO_3 (2.284 g, 21.549 mmol). The mixture was further heated (80 °C) and stirred for 15 h. After cooling, the solution was filtered and the solvent was removed under vacuum yielding an off-white solid (2.073 g, 6.947 mmol, 97%). ^{13}C NMR ($CDCl_3$): δ 171.8 (−NH−CO); 66.7 (−O−CH_2−); 62.1, 57.4, 55.9 (−N−CH_2−); 39.1 (N−CH_2–CO); 29.8, 27.7 (−CH_2−). MS (CI): *m*/*e* 299 (M + 1), 327 (M + 29), 339 (M + 41).

14-Oxa-1,4,8,11-tetraazabicyclo[9.5.3]nonadecane (L1). A solution of BH_3·THF (100 mL; 1 M in THF) was added to a slurry of H_2L2 (1.002 g, 3.358 mmol) in dry THF (30 mL), and the mixture was refluxed for 24 h under N_2. Water (5 mL) was added dropwise to the ice-cooled solution to destroy the excess BH_3. Removal of solvents (in vacuo) yielded a white solid residue, which was refluxed in HCl (6 M, 40 mL) for 3 h. After cooling and basification to pH 14 with KOH, the product was extracted with chloroform (6 × 50 mL), dried over K_2CO_3, filtered, and rotoevaporated to dryness yielding a colorless oil (0.772 g, 2.855 mmol, 85%). ^{13}C NMR ($CDCl_3$): δ 73.2 (−O−CH_2–); 58.1, 57.7, 56.5, 47.5, 47.1 (−N−CH_2–); 27.9, 27.8 (aliphatic CH_2–). MS (CI): *m*/*e* 271 (M + 1), 299 (M + 29), 311 (M + 41).

(1,4,8,11-Tetraaza-14-oxabicyclo[9.5.3]nonadecane)nickel(II) perchlorate. Ligand L1 (0.258 g, 0.954 mmol) was dissolved in dry ethanol (30 mL), and an excess of nickel(II) acetate tetrahydrate (0.950 g, 3.816 mmol) was added with stirring. The mixture was refluxed overnight under N_2, and after cooling, a fine green precipitate of unreacted nickel(II) acetate was centrifuged off, leaving an intensely purple supernatant. Solvent was removed under vacuum, and the resulting solid was dissolved in water (15 mL) and purified on Sephadex CM C-25 cation-exchange resin using 0.1 and 0.2 M $NaClO_4$ as eluant. Only a single moving purple band and a stationary green band ($Ni(H_2O)_6^{2+}$) were observed. After reduction of the volume of the purple solution, while still hot (ca. 60 °C), it was placed in an ice bath resulting in the precipitation of a pale purple product. This material was recrystallized by diffusion of diethyl ether into a nitromethane solution of the complex, filtered, washed with ethanol and diethyl ether, and air-dried. Yield: 199 mg (40%).

MS (+ve FAB, mNBA): 427 = $[Ni(L1)ClO_4)]^+$, 327 = $[Ni(L1-H)]^+$. Calcd for $[Ni(C_{14}H_{30}N_4O)(ClO_4)](ClO_4)$: C, 31.85; H, 5.73; N, 10.61. Found: C, 31.48; H, 5.75; N, 10.41%.

(1,4,8,11-Tetraaza-14-oxabicyclo[9.5.3]nonadecane-3,9-dione)nickel(II) perchlorate. A solution containing $Ni(ClO_4)_2$·$6H_2O$, (0.122 g, 0.335 mmol) and ligand H_2L2 (0.100 g, 0.335 mmol) was prepared in dry methanol (25 mL), and the mixture was refluxed for 1 h under N_2. The solution turned a maroon color, and a green precipitate developed which was filtered off. The filtrate was adjusted to pH 7 with aqueous 0.1 M NaOH, and the maroon complex was precipitated by slow diffusion of diethyl ether into the neutral complex solution. The monodeprotonated product was recrystallized by slow evaporation of an acetonitrile solution, and the complex was filtered, washed with diethyl ether, and air-dried. Yield: 30 mg (19%). MS (+ve FAB): 455 = $[Ni(H_2L2)(ClO_4)]^+$, 355 = $[Ni(HL2)]^+$. Calcd for $[Ni(C_{14}H_{25}N_4O_3)(ClO_4)]$·$H_2O$: C, 35.51; H, 5.75; N, 11.83. Found: C, 35.80; H, 4.99; N, 11.82%.

Crystallography. $[Ni(L1)(ClO_4)](ClO_4)$. X-ray quality crystals were grown by slow evaporation of an aqueous solution containing the complex and $NaClO_4$. The experimental parameters are listed in Table 1.

A pale pink plate crystal of dimensions 0.40 × 0.45 × 0.05 mm was mounted on a glass fiber and optically centered in a Rigaku AFC6S diffractometer employing graphite-monochromated Mo Kα radiation and a 2 kW sealed tube generator. The unit cell was refined using 25 reflections in the 2θ range 8.73−31.27°. The diffraction data were collected at 26 ± 1 °C using the $\omega-2\theta$ scan technique to a maximum 2θ value of 50.1°. A total of 4214 reflections were collected, 3941 of which were unique. An empirical absorption correction, using the program DIFABS,[16] was applied which resulted in transmission factors ranging from 0.72 to 1.50. This structure was determined some time ago, being one of the last using DIFABS. The absorption correction is small, and no obviously anomalous anisotropic effects were generated. The data were corrected for Lorentz and polarization effects. The

(12) Donnelly, M. A.; Zimmer, M. *Inorg. Chem.* **1999**, *38*, 1650.
(13) Hambley, T. W. *J. Chem. Soc., Chem. Commun.* **1984**, 1228.
(14) Atkins, T. J.; Richman, J. E.; Oettle, W. F. *Org. Synth.* **1978**, *58*, 86.
(15) Bradshaw, J. S.; Krakowiak, K. E.; Izatt, R. M. *J. Heterocycl. Chem.* **1989**, *26*, 1431.
(16) DIFABS: Walker, N.; Stuart, D. *Acta Crystallogr.* **1983**, *A39*, 158−166.

Table 1. Crystallographic Data for Macrobicyclic Complexes

empirical formula	$C_{14}H_{30}N_4O_9Cl_2Ni$	$C_{14}H_{24}ClN_4NiO_7$
mol wt	528.02	454.52
space group	*P*21/*c* (no. 14)	*Pbca* (no. 61)
a/Å	8.608(3)	15.1590(3)
b/Å	16.618(3)	13.235(2)
c/Å	14.924(4)	18.0195(6)
β/deg	91.53(3)	90
V/Å	2134(1)	3615.3(7)
Z	4	8
D_{calc}/g·cm^{-3}	1.643	1.670
μ/Å	0.71069	0.71069
μ/cm^{-1}	12.16	12.68
no. params	307	265
R	0.050	0.045
R_w	0.046	0.083

[a] $R = \sum\%F_o| - |F_c\%/\sum|F_o|$; $wR_2 = [(\sum w(F_o^2 - F_c^2)^2/\sum w(F_o^2)^2]^{1/2}$.

structure was solved by direct methods.[17a,b] The non-hydrogen atoms were refined anisotropically. Neutral scattering factors were taken from Cromer and Weber.[18a] Anomalous dispersion effects were included in F_{calc},[18b] the values for $\Delta f'$ and $\Delta f''$ were those of Creagh and McAuley[18c] and the mass attenuation coefficients presented by Creagh and Hubbell.[18d] All calculations were performed using the teXsan[18e] crystallographic software package of Molecular Structure Corporation. The final cycle of full-matrix least-squares refinement was based on 2702 observed reflections with $I > 2.00\sigma(I)$ and 307 variable parameters and converged (largest parameter shift was 0.00 times its estimated standard deviation (esd)) at $R = 0.050$ ($R_w = 0.046$). Maximum and minimum peaks on the final difference Fourier map were 0.640 and −0.35 e Å^{-3}, respectively.

[Ni(HL2)](ClO$_4$). Crystals were grown by slow evaporation of a solution of the complex in MeCN, and the experimental parameters are provided in Table 1. A pink plate crystal of approximate dimensions 0.02 × 0.15 × 0.20 mm was mounted on a glass fiber. All measurements were made on a Rigaku/ADSC CCD area detector with graphite monochromated Mo Kα radiation. The data were collected at −93 ± 1 °C to a maximum 2θ value of 61.0°. Data were collected in 0.50° oscillations with 80.0 s exposures. A sweep of data was done using φ oscillations from 0.0 to 190.0° at $\chi = -90°$, and a second sweep was performed using ω oscillations between −23.0° and 18.0° at $\chi = -90°$. The structure was solved by heavy atom Patterson methods[19]and expanded using Fourier techniques.[17b] There is substantial disorder in the ligand which was partially resolved by split-atom refinement of O(3), C(9), C(13), and C(14). Additional atoms of the ligand are probably disordered, but they could not be resolved and O(3a), C(13a), and C(13) were refined isotropically (non-positive-definite when anisotropic), while the remaining non-hydrogen atoms were refined anisotropically. Hydrogen atoms were fixed in calculated positions with C−H = 0.98 Å and thermal parameters 1.2 times those of the parent atoms. Neutral scattering factor anomalous dispersion effects, the values for $\Delta f'$ and $\Delta f''$, mass attenuation coefficients, and calculations were performed as described above.[18] The final cycle of full-matrix least-squares refinement was based on all 5137 unique reflections and 265 variable parameters and converged (largest parameter shift was 0.02 times its esd) with unweighted and weighted agreement factors of $R_1 = 0.045$ and $wR_2 = 0.083$. Maximum and minimum peaks on the final difference Fourier map corresponded to 1.33 and −1.63 e Å^{-3}, respectively.

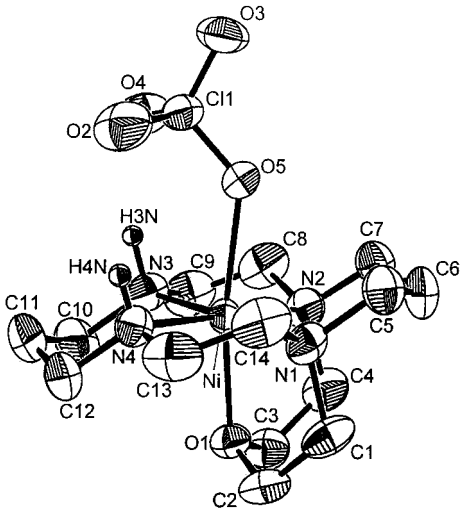

Figure 1. ORTEP diagram of the cation $[Ni(L1)(ClO_4)]^+$, showing 25% thermal ellipsoids.

Table 2. Selected Interatomic Distances (Å) and Bond Angles (deg) for $[Ni(L1)(ClO_4)](ClO_4)$

Interatomic Distances			
Ni(1)−O(1)	2.094(3)	Ni(1)−N(2)	2.079(4)
Ni(1)−O(1)	2.252(4)	Ni(1)−N(3)	2.066(5)
Ni(1)−N(1)	2.078(4)	Ni(1)−N(4)	2.065(4)
Bond Angles			
O(1)−Ni(1)−O(5)	170.2(1)	O(5)−Ni(1)−N(4)	91.3(2)
O(1)−Ni(1)−N(1)	84.5(2)	N(1)−Ni(1)−N(2)	95.2(2)
O(1)−Ni(1)−N(2)	84.4(2)	N(1)−Ni(1)−N(3)	178.5(2)
O(1)−Ni(1)−N(3)	95.3(2)	N(1)−Ni(1)−N(4)	85.8(2)
O(1)−Ni(1)−N(4)	94.7(2)	N(2)−Ni(1)−N(3)	86.2(2)
O(5)−Ni(1)−N(1)	88.3(2)	N(2)−Ni(1)−N(4)	178.6(2)
O(5)−Ni(1)−N(2)	89.7(2)	N(3)−Ni(1)−N(4)	92.8(2)
O(5)−Ni(1)−N(3)	92.0(2)		

[a] Estimated standard deviations in the least significant figure are given in parentheses.

Results and Discussion

The macrocycle [10]-aneN_2O (**1**) was synthesized as described previously.[20] Reaction of 1,3-diaminopropane with 2 equiv of chloroacetyl chloride yielded the clawlike diamide (**2**) similar to that prepared previously by Bradshaw.[15,21] The reaction of the bis-amide (**2**) with **1** in the presence of base in dry acetonitrile yielded the ligand H_2L2. Subsequent reduction of the cyclic amides gave the macrobicyclic ligand L1.

Molecular Structure. An ORTEP presentation of the $[Ni(L1)(ClO_4)]^{2+}$ ion is shown in Figure 1. Selected bond lengths and bond angles are provided in Table 2. Atomic coordinates and other parameters are provided in Supplementary Tables S1−S3. The geometry around the nickel center is only slightly distorted from an ideal octahedron, with the L1 ligand donors occupying five coordination sites and a perchlorate ion the other. Ligand L1 can be envisaged as the fusion of a 10-membered cyclodecane ring with a 14-membered cyclotetradecane ring where substituents on the nitrogens adopt the *trans*-III config-

(17) (a) MITHRIL: C. J.Gilmore, *J. Appl. Crystallogr*. **1984**, *17*, 42−46. (b) DIRDIF94: Beurskens, P. T.; Admiral, G.; Beurskens, G.; Bosman, W. P.; de Gelder, R.; Israel, R.; Smits, J. M. M. *The DIRDIF-94 program system*; Technical Report of the Crystallography Laboratory, University of Nijmegen, The Netherlands, 1994.

(18) (a) Cromer, D. T.; Weber, J. T. *International Tables for X-ray Crystallography*; The Kynoch Press: Birmingham, England, 1974; Vol. IV, Table 2.2 A. (b) Ibers, J. A.; Hamilton, W. C. *Acta Crystallogr*. **1964**, *17*, 781. (c) Creagh, D. C.; McAuley, W. J. *International Tables for Crystallography*; Wilson, A. J. C., Ed.; Kluwer Academic Publishers: Boston, 1992; Vol. C, Table 4.2.6.8, pp 219−222. (d) Creagh, D. C.; Hubbell, J. H. *International Tables for Crystallography*; Wilson, A. J. C., Ed.; Kluwer Academic Publishers: Boston, 1992; Vol. C, pp 200−206. (e) teXsan: Crystal Structure Analysis Package, Molecular Structure Corporation, 1985 and 1992.

(19) PATTY: Beurskens, P. T.; Admiraal, G.; Beurskens, G.; Bosman, W. P.; Garcia-Granda, S.; Gould, R. O.; Smits, J. M. M.; Smykalla, C. The DIRDIF program system; Technical Report of the Crystallography Laboratory, The University of Nijmegen, 1992.

(20) Chandrasekhar, S.; McAuley, A. *J. Chem. Soc., Dalton Trans*. **1992**, 2967.

(21) Coulter, K. Ph.D. Dissertation, University of Victoria, 1997.

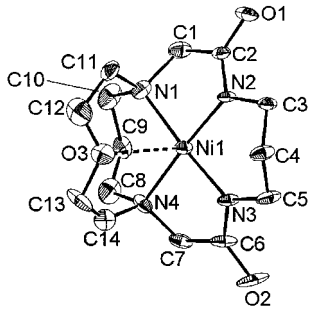

Figure 2. ORTEP diagram of the cation $[Ni(HL2)]^+$, showing 25% thermal ellipsoids.

uration according to Bosnich et al..[7] Numerous studies on such complexes indicate that the *trans*-III configuration is the most stable. In contrast to $[Ni(L1)(ClO_4)]^{2+}$, the *trans*-I configuration is adopted[8−11] in the macrobicyclic ions $[M(L3)]^{2+}$ and $[M(L4)(ClO_4)]^{2+}$ (M = Ni(II), Cu(II)) and $[Co(L4)(CH_3CN)]^{3+}$.[21] The ligands L3 and L4 are structural isomers of L1 which form complexes that cannot adopt the *trans*-III configuration. Molecular mechanics calculations indicate that the *trans*-I configuration has a significantly smaller best-fit metal−nitrogen bond distance of 2.01 Å than the *trans*-III (2.07 Å).[22] The ideal high spin Ni(II)−nitrogen bond distance is approximately 2.10 Å.[23] In $[Ni(L1)(ClO_4)]^{2+}$, the Ni(1)−N bond distances range from 2.065 to 2.079 Å, consistent with little ligand strain. There is a slight distinction between the Ni(1)−N(tertiary) and Ni(1)−N(secondary) bond distances with the former slightly longer as expected due to increased steric repulsion at the tertiary nitrogens. The shorter Ni(1)−O(ether) distance of 2.094 Å with respect to the Ni(1)−O(perchlorate) distance of 2.252 Å reflects the stronger binding of the apical ether oxygen in the solid. These Ni−O bond distances are both shorter than the corresponding bonds in the $[Ni(L3)(ClO_4)]^{2+}$ cation [2.109 Å, Ni−O(ether) and 2.373 Å, Ni−O(perchlorate)]. Also, the *trans*-basal angles N(1)−Ni(1)−N(3) and N(2)−Ni(1)−N(4) are 178.5(2)° and 178.6(2)°, respectively. These are slightly larger and closer to 180° than those observed in the corresponding $[Ni(L3)(ClO_4)]^{2+}$ cation (177.4° and 178.0°, respectively), confirming that in $[Ni(L1)(ClO_4)]^{2+}$ the metal ion sits within the N_4 plane. The Ni−O(1) vector shows only a slight deviation (5.5°) from perpendicularity with the N_4 plane owing to the better encapsulation of the nickel into the N_4 plane. The *trans*-III configuration may facilitate formation of hydrogen bonds between the protons attached to the secondary nitrogens and the oxygen atoms of the bonded ClO_4^- (N(3)−H(3N) = 1.002 Å, N(4)−H(4N) = 0.830 Å).

In Figure 2 the structure of $[Ni(HL2)]^+$ is shown. Important bond lengths and angles are presented in Table 3, and atomic coordinates and other parameters are provided in Supplementary Tables S4−S6. At the pH used for isolation, one of the amide residues is deprotonated, resulting in a singly charged ion. Unlike in $[Ni(L1)(ClO_4)]^{2+}$, owing to the strong ligand field of the amides, this ion is now better described as square planar with weak interactions between the metal center, the apical oxygen (Ni(1)−O(3) = 2.651 Å), and an oxygen (Ni(1)−O(3a) = 2.451 Å) of an adjacent ligand. The nickel atom is located only slightly above (0.006 Å) the plane of the four nitrogen donors (mean deviation of all atoms = 0.0386 Å). As anticipated, the metal ion−amide nitrogen bonds are considerably shorter than those to the tertiary nitrogens. The Ni(1)−O(3) vector deviates 13° from perpendicular, considerably larger than the corresponding angle for the fully saturated system. The vector to atom O(3a) is displaced 8.2° from normal, thereby creating a zigzag pattern throughout the lattice.

Table 3. Selected Interatomic Distances (Å) and Bond Angles (deg) for $[Ni(HL2)](ClO_4)$

Interatomic Distances			
Ni(1)−O(3)	2.651(6)	Ni(1)−O(3a)	2.451(12)
Ni(1)−N(1)	1.983(3)	Ni(1)−N(2)	1.889(3)
Ni(1)−N(3)	1.872(3)	Ni(1)−N(4)	1.970(3)
Bond Angles			
O(3)−Ni(1)−N(1)	77.0(2)	O(3)−Ni(1)−N(2)	108.3(2)
O(3)−Ni(1)−N(3)	108.1(2)	O(3)−Ni(1)−N(4)	74.4(2)
O(3a)−Ni(1)−N(1)	81.8(3)	O(3a)−Ni(1)−N(2)	98.3(3)
O(3a)−Ni(1)−N(3)	103.1(3)	O(3a)−Ni(1)−N(4)	84.1(3)
N(1)−Ni(1)−N(2)	83.89(14)	N(1)−Ni(1)−N(3)	174.77(15)
N(1)−Ni(1)−N(4)	99.14(13)	N(2)−Ni(1)−N(3)	93.32(12)
N(2)−Ni(1)−N(4)	176.42(14)	N(3)−Ni(1)−N(4)	83.51(14)

Solution Studies. The UV−visible spectrum of $[Ni(L1)(OH_2)]^{2+}$ exhibited a charge-transfer band at 197 nm ($\epsilon = (6.1 \pm 0.2) \times 10^3$ M^{-1} cm^{-1}) and four d−d transitions at 334 nm ($\epsilon = 11$ M^{-1} cm^{-1}), 505 nm (6 M^{-1} cm^{-1}), 675 nm (3 M^{-1} cm^{-1}), and 1059 nm (3 M^{-1} cm^{-1}). The presence of a band at $\lambda >$ 1000 nm can be best interpreted in terms of strong tetragonal distortion as demonstrated in the crystal structure. The in-plane ligand field strength, Dq^{xy}, is 1482 cm^{-1}, similar to that for the geometric isomer $[Ni(L3)(OH_2)]^{2+}$ (1468 cm^{-1}). Therefore, the difference in position of the ether bridge in L1 and L3 does not significantly increase the ligand field of the macrobicycle. Also, Busch et al.[24] have shown that for the *trans*-$[Ni([14]aneN_4)X_2]$ series, X = halide, Dq^{xy} has an average value of 1460 cm^{-1}. Thus, conversion of two secondary nitrogens to tertiary donors does not appear to result in any substantial change to the in-plane ligand field.

The principal features in the UV−visible spectrum of $[Ni^{III}(L1)(H_2O)]^{3+}$ are the charge-transfer bands at 315 nm ($\epsilon = 3.7 \times 10^3$ M^{-1} cm^{-1}) and 390 nm ($\epsilon = 3.0 \times 10^3$ M^{-1} cm^{-1}). Small differences in the spectra were observed when $[H^+]$ was varied from 0.004 to 0.3 M suggestive of a proton equilibrium. Use was made of this feature in determining a pK_a within this acidity range. Absorbance changes (ΔA) were monitored (Supplementary Figure S1) over the range 200−450 nm when microliter aliquots of perchloric acid (4.0 M) were added sequentially to a $[Ni(L1)]^{3+}$ solution starting at $[H^+] = 0.004$ M. From ΔA_{320} (Figure 3), a $pK_a = 0.034 \pm 0.04$ was derived. Results of an identical experiment on $[Ni(cyclam)(H_2O)_2]^{3+}$ showed no similar behavior (see Figure 3), confirming the involvement of the ether oxygen in the equilibrium (vide infra).

EPR Spectroscopy. Yellow/green aqueous solutions of the $[Ni(L1)(OH_2)]^{3+}$ complex were prepared by oxidation of $[Ni(L1)]^{2+}$ with excess sodium persulfate. The spectra (Supplementary Figure S2) are consistent with a low-spin d^7 cation in a distorted-octahedral environment[25] with $g_\perp = 2.200$ and $g_\parallel = 2.028$. No evidence of hyperfine interaction was observed. Addition of Et_4NCl resulted in $[Ni(L1)(Cl)]^{3+}$ formation, with $g_\perp = 2.184$, $g_\parallel = 2.028$, and $A_\parallel = 30$ G. The four line splitting at $g_\parallel$ is consistent with a chloride ion in the coordination sphere. In an attempt to displace the axial ether oxygen atom from the

(22) Boeyens, J. C. A.; Dobson, S. M.; Hancock, R. D. *Inorg. Chem.* **1985**, *24*, 3073.

(23) Thöm, V. J.; Fox, C. F.; Boeyens, J. C. A.; Hancock, R. D. *J. Am. Chem. Soc.* **1984**, *106*, 5947. Adam, K. R.; Antolovich, M.; Brigden, L. G.; Lindoy, L. F. *J. Am. Chem. Soc.* **1991**, *113*, 3346.

(24) Martin, L. Y.; Sperati, C. R.; Busch, D. H. *J. Am. Chem. Soc.* **1977**, *99*, 2968.

(25) Haines, R. I.; McAuley, A. *Coord. Chem. Rev.* **1981**, *39*, 77. Gore, E. S.; Busch, D. H. *Inorg. Chem.* **1973**, *12*, 1.

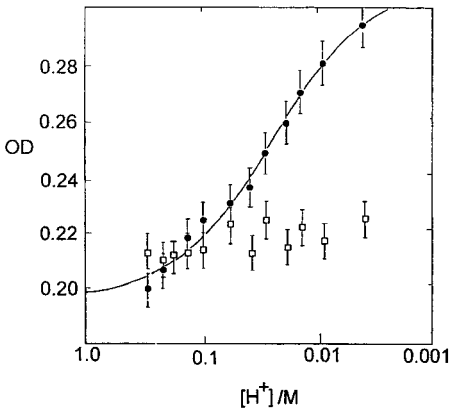

Figure 3. Spectrophotometric titration ($\lambda = 320$ nm) of $[Ni(III)(L1)(OH_2)]^{3+}$ with $HClO_4$, at $[H^+] = 0.004-0.3$ M (filled circles). For comparison, the corresponding data for $[Ni(III)(cyclam)(OH_2)_2]^{3+}$ over the same range are presented (open boxes).

Table 4. Electrochemical Measurements (V) in CH_3CN, 1 M TBAP, vs Ag/AgCl

ligand	Ni(III)/Ni(II)	Ni(II)/Ni(I)
L1	0.85[a]	1.53[c]
L2	0.24[b]	1.19[c]
L3	0.86 [a]	1.64[b]
cyclam	0.59[a]	

[a] Reversible. [b] Quasi-reversible. [c] Irreversible.

first coordination sphere, 6 M $HCl_{(aq)}$ was added to $[Ni(L1)(H_2O)]^{3+}$. However, no further change in the EPR spectrum was observed. Although at room temperature a dichloro complex is expected, the result of freezing the solution is considered to promote reinforcement of the ether oxygen coordination as has been observed previously.[26] The spectra are similar to those of related isomeric ions based on L3, where for the aqua ion the *g* values are identical, but for the chloro complex, values of 2.160, 2.024, and 22 G were derived.

Electrochemistry. At 100 mV/s, the cyclic voltammogram of $[Ni(L1)(ClO_4)](ClO_4)$ in acetonitrile at 25 °C displayed a single reversible $Ni^{III/II}$ wave at 0.85 V (vs Ag/Ag^+), while an irreversible cathodic peak is observed at -1.53 V for the $Ni^{II/I}$ reduction. It can be seen from Table 4 that the behavior of $[Ni(L1)(solv)]^{2+}$ is very similar to that of $[Ni(L3)(solv)]^{2+}$ with no greater stabilization of the Ni(III) ion. The $E_{1/2}$ of $[Ni(L1)]^{3+/2+}$ is substantially larger[28] than that of $[Ni(cyclam)]^{3+/2+}$. This is consistent with the conversion of two secondary amines to tertiary amines that are known to stabilize lower oxidation states. Kimura et al.[27] observed that a wide range of oxo-polyamine macrocyclic ligands stabilize Ni(III) thermodynamically with lower redox potentials than their saturated analogues. In the case of $[Ni(HL2)]^+$, the diamide ligand imparts an extra stabilization of 610 mV on the Ni(III) complex over the saturated derivative L1. The lower $E_{1/2}$ of the $[Ni(HL2)]^{2+/+}$ couple can be attributed to the electron delocalization at the amide nitrogens favoring the more electron deficient Ni(III) and to the deprotonated amides being stronger in-plane donors.

Kinetic Studies. No decomposition of $[Ni(L1)]^{2+}$ in 1 M $HClO_4$ was observed at 520 nm over 12 h. In the case of $[Ni(L1)(solv)]^{3+}$, at $[H^+] = 0.008$ M, the rate constant for decomposition at 10 °C was $(1.43 \pm 0.08) \times 10^{-3}$ s^{-1}, and under these conditions, the complex is sufficiently long-lived to undertake substitution experiments. The decomposition rate is invariant with $[H^+]$ over the range 1.0−0.05 M. At lower hydrogen ion levels, base-catalyzed pathways[28] become operative. It is of interest that the mode of decomposition differs from that of $[Ni(III)cyclam(H_2O)_2]^{3+}$, where an increasing decomposition rate is observed with a uniform increase in pH.[29]

Scheme 1

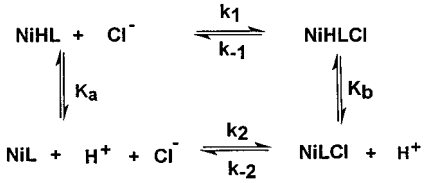

Chloride Substitution Reactions. Substitution reactions at Ni(III) centers have been studied previously, with four-coordinate cyclam-based ligands,[29,30] and dissociative interchange mechanisms have been proposed. The rate of substitution at $[Ni(L1)(OH_2)]^{3+}$ was found to be both chloride and hydrogen ion dependent. Substitution kinetics were investigated between $[H^+] = 0.12-1.0$ M with $[Cl^-]$ approximately 10−40 times those of [Ni(III)]. Complete rate data, monitored at either 310 or 420 nm, are presented in Supporting Information (Table S7). In general, the scatter of individual values for k_{obs} was on the order of 5%. The chloride complex is considerably less reactive than the aqua species, persisting at room temperature for several hours. Increased kinetic inertness, observed for other Ni(III) macrocyclic complexes with axial chloride,[29] is probably associated with the lower redox potential observed. At constant $[H^+]$, first-order rate constants (k_{obs}) vary linearly with $[Cl^-]$. Scheme 1 is presented, consistent with the observed $[H^+]$ and $[Cl^-]$ dependences, where (neglecting charges) NiHL and NiL represent the complex ions $[Ni(L1)(OH_2)(OH_3)]^{4+}$ and $[Ni(L1)(OH_2)_2]^{3+}$ and $NiH(L1)Cl^{3+}$ and $[Ni(L1)Cl]^{2+}$ represent the corresponding chloro complexes $[Ni(L1)(OH_3)Cl]^{3+}$ and $[Ni(L1)(OH_2)(Cl)]^{2+}$.

The rate law derived from this scheme may be represented as

$$k_{obs} = \frac{k_1[H^+] + k_2K_a}{K_a + [H^+]}[Cl^-] + \frac{k_{-1}[H^+] + k_{-2}K_b}{K_b + [H^+]} \quad (1)$$

Complex inverse $[H^+]$ dependences are predicted for both the intercepts and slopes of plots of k_{obs} vs $[Cl^-]$. However, in studies undertaken at 5.5, 10, and 25 °C, (Supporting Information Table S7, supplementary figures S3−S8), only at 25 °C was any consistent variation of intercept with $[H^+]^{-1}$ observed. A global least-squares treatment of the data at each temperature was attempted but was not successful, probably owing to the significant numerical differences between the slope and intercept terms. Therefore, a treatment was used where slopes and intercepts were examined separately. From eq 1 it may be observed that plots of $\{\text{slope}(K_a + [H^+])\}$ vs $[H^+]$ and $\{\text{intercept}(K_b + [H^+])\}$ vs $[H^+]$ should yield individual rate constants. Assuming $K_a = K_b$ and using the value of K_a determined spectrophotometrically from the scheme, K_1 and K_2 should be equal. At 5.5 °C, the intercepts (0.068 ± 0.005) of the k_{obs} vs $[Cl^-]$ curves (supplementary data) were constant over

(26) Lappin, A. G.; Margerum, D. W. *Inorg. Chem.* **1978**, *17*, 1630.
(27) Machida, R.; Kimura, E.; Kushi, Y. *Inorg. Chem.* **1986**, *25*, 3461. Kimura, E.; Anan, H.; Koike, T.; Shiro, M., *J. Org. Chem*. **1989**, *54*, 3998.
(28) Sonnberger, B.; Huhn, P.; Wasserburger, A.; Wasgestian, F. *Inorg. Chim. Acta* **1992**, *196*, 65.
(29) Haines, R. I.; McAuley, A. *Inorg. Chem.* **1980**, *19*, 719.
(30) Zeigerson, E.; Ginsburg, G.; Schwartz, N.; Luz, Z.; Meyerstein, D. *J. Chem. Soc., Chem. Commun*. **1979**, 241.

the hydrogen ion range used, and no significant differences were observed with $[H^+]$ in the function $\{\text{slope}(K_a + [H^+])\}$ (10.1 ± 1.2), suggestive of only one pathway, attributable to k_2K_a ($k_2 \approx 300 \pm 50\ M^{-1}\ s^{-1}$). At 10.0 °C, the intercepts from plots of k_{obs} vs $[Cl^-]$ were again essentially constant ($C = 0.075 \pm 0.02$), but variation of slopes with $[H^+]$ yielded $k_1 = 7.4 \pm 3.5\ M^{-1}\ s^{-1}$ and $k_2K_a = 9.0 \pm 1.5\ s^{-1}$ ($k_2 = 265 \pm 50\ M^{-1}\ s^{-1}$) within error essentially constant over the small temperature range. At 25 °C, however, by use of the functions identified, values of $k_1 = 142 \pm 30\ M^{-1}\ s^{-1}$ and $k_2K_a = 48 \pm 18\ s^{-1}$ ($k_2 = 1400 \pm 350\ M^{-1}\ s^{-1}$) and $k_{-1} = 0.22 \pm 0.08\ s^{-1}$ and $k_{-2}K_b = 0.09 \pm 0.05\ M^{-1}\ s^{-1}$ ($k_{-2} = 2.7 \pm 1.5\ M^{-1}\ s^{-1}$) were obtained. In this case, values of K_1 (645 ± 600 M) and K_2 (530 ± 700 M) are essentially the same as predicted by the mechanism. The large uncertainties in the data reflect the relative instability of the nickel(III) species, especially at lower proton concentrations.

Origin of the Protonation Equilibria for the Substitution Reaction. There is a significant difference between the present findings and those for the corresponding $[Ni(cyclam)(H_2O)_2]^{3+}$ species,[29] although rate data for Cl^- substitution were determined over approximately the same $[H^+]$ range (0.004−0.30 M). In the latter case, there is no evidence of any $[H^+]$ dependence, in keeping with a relatively high (>3) pK_a value for protolysis of the first aqua ligand.[30] In the present investigation, the initial substitution occurs at a much higher acid concentration, reflecting an additional process at the metal center. If the ether oxygen remained bound, and the aqua ion in the sixth site was deprotonated, it is unlikely that the chloride ion would more readily replace the resultant hydroxo ion than water in the inner coordination sphere. Additionally, the reaction rate increases as the pH rises, again inconsistent with a complexed hydroxo ion as a reactant. It is known that binding between transition metal ions and ether oxygen donors is generally weak. A possible reaction mechanism involves an incoming H_3O^+ that induces the detachment of the axial ether O donor and its simultaneous protonation with hydrogen bonding to the ether and also coordination to the nickel center. It is considered that in this process there is an overall increase in the charge at the metal center resulting in a more tightly bound *trans*-water. Release of H^+ from the ether-bound H_3O^+, as shown below, would then provide a less tightly held water molecule. In such circumstances, increased lability of the latter water molecule would be anticipated, consistent with the increase in rate with $[H^+]^{-1}$ observed. The present results confirm this proposal, where in all cases the k_2 value exceeds that of k_1. The much more inert cobalt(III) ion crystallizes as $[Co(L3)(H_2O)]^{3+}$, but in solution this ion is postulated to coordinate two water molecules as described here. Observations[31] in this laboratory have identified two pK_a values at 2.2 ± 0.2 and 3.8 ± 0.2 consistent with two sequential H^+ dissociations at both trans-disposed sites, providing evidence for behavior similar to that outlined above.

In the case of nickel(II) cyclam, Pierce et al.[32] have shown that oxidation of the *trans*-I form results in the formation of a transient *trans*-I nickel(III) complex which rearranges rapidly to the *trans*-III configuration. In the present system, the presence

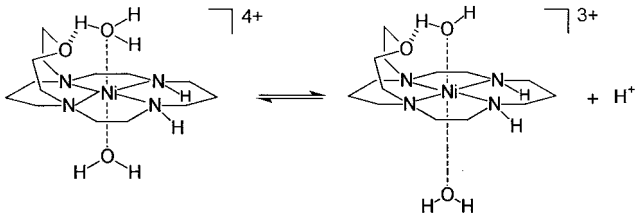

of the ether O that can accept a protonated water molecule is considered essential for the hydrogen ion dependences observed. The lack of any comparable donor in the case of the cyclam system would explain the observed differences in reactivity. It is of interest to note that a similar acid/base equilibrium has been observed in hydroxo donor pendant armed nickel(II) macrocycles.[33] In this instance, the pK_a values are less than unity for the detachment and protonation of the pendant hydroxo arm, probably reflecting the greater interaction of the negatively charged oxygen donor and the nickel center than is the case in the present study.

In addition to the different acidity profile observed here, although the equilibrium constants are roughly similar, the rate constants for chloride substitution at 6.6 °C on $[Ni(III)cyclam(H_2O)_2]^{3+}$, $k_1 = 168 \pm 5\ M^{-1}\ s^{-1}$ and $k_{-1} = 1.15 \pm 0.10\ s^{-1}$ ($K_1 = 146$ M) are substantially larger than in the present system ($k_1 = 8 \pm 5\ M^{-1}\ s^{-1}$, $T = 10.0$ °C). The current investigation indicates differences in the mode of replacement of the coordinated water by the halide. Clearly, further work is required to examine these effects.

Acknowledgment. We acknowledge the award of a Natural Sciences and Engineering Research Council (NSERC) International Fellowship to T.R. and the continued funding of this research by the University of Victoria and NSERC, Canada. The experimental assistance of Paul Servin, financial support from the Swedish Natural Science Research Council, and a Visiting Professorship grant from the Wenner Gren Foundation, Stockholm, to A.McA. are gratefully acknowledged. We appreciate helpful discussions with Drs. David Harrington and Reg Mitchell and S. Subramanian.

Supporting Information Available: Tables S1−S6, containing bond distances, angles, anisotropic thermal parameters, selected intermolecular distances (17 pages). Table S7, listing rate data for the substitution process, and Table S8, treatment of intercepts and slopes from k_{obs} vs $[Cl^-]$ plots (3 pages). Figure captions and Figures S1 illustrating the hydrogen ion dependence of the UV−vis spectra, Figures S2a and S2b the EPR spectra of the $[Ni(III)(L1)]^{3+}$ ion and $[Ni(III)(L1)(Cl)]^{2+}$, and Figures S3−S8, plots of k_{obs} vs $[Cl^-]$ and treatment of the slopes and intercepts (9 pages). This material is available free of charge via the Internet at http://pubs.acs.org. A complete X-ray report on $[Ni(L1)(ClO_4)](ClO_4)$ (38 pages with structure factor tables 26 pages) is available in hard copy only. A CIF file on $[Ni(HL2)](ClO_4)$ has been deposited.

IC001163R

(31) Ishihara, K.; McAuley, A. Unpublished observations.
(32) Pierce, D. T.; Hatfield, T. L.; Billo, E. J.; Ping, Y. *Inorg. Chem.* **1997**, *36*, 2950.
(33) Lotz, T. J.; Kaden, T. A. *Helv. Chim. Acta* **1978**, *61*, 1376.